Computational Materials Science 153 (2018) 461–472

Contents lists available at ScienceDirect

Computational Materials Science

journal homepage: www.elsevier.com/locate/commatsci

Electronic properties of RX_2Al_{20} (R = La, Ce, Yb, Th, U; X = Ti, V, Cr and Mn) cage compounds

Przemysław Swatek[a,b,c,*], Maja Kleinert[a], Piotr Wiśniewski[a], Dariusz Kaczorowski[a]

[a] Institute of Low Temperature and Structure Research, Polish Academy of Sciences, Wrocław, Poland
[b] Division of Materials Science and Engineering, Ames Laboratory, Ames, Iowa 50011, USA
[c] Department of Physics and Astronomy, Iowa State University, Ames, Iowa 50011, USA

ARTICLE INFO

Keywords:
Rare earth intermetallics
Caged compounds
Orbital hybridization
Electronic band calculations
Fermi surface
Quantum oscillations

ABSTRACT

Non-spin-polarized electronic structures and Fermi surface properties of RX_2Al_{20} (R = La, Ce, Yb, Th, U; X = Ti, V, Cr, Mn) intermetallic compounds were calculated using the full potential all-electron local orbital (FPLO) approach in the framework of the local density approximation (LDA). Trends of the magnetism are discussed in terms of the characteristics of X-3d bands with a quantitative analysis of the relationship between band electron filling and crystal electric field splitting. Since coordination icosahedra of X-atoms have small trigonal distortion, crystal electric field splits the fivefold degenerate X-3d state into low-energy singlet a_{1g} and two higher-energy doublets e_g. In RTi_2Al_{20} and RV_2Al_{20} the population of the related 3d sub-band is not sufficient to cause energetically favorable spin polarization, whereas magnetic instabilities develop in the RCr_2Al_{20} series. Finally, a manifestation of strong repulsive interactions between itinerant Mn-d electrons become most pronounced in ferromagnetic UMn_2Al_{20}. The influence of non-magnetic R-f states on magnetic and thermodynamic properties is discussed with special emphasis on the role of the f–p and f–d hybridization. For $LaTi_2Al_{20}$ and LaV_2Al_{20} the calculated quantum oscillation frequencies are in accord with experimental reports.

1. Introduction

The large family of ternary intermetallics with the general composition RT_2M_{20}, where R = rare earth or U, T = 3d, 4d or 5d-electron transition metal, and M = Zn, Cd or Al, comprises an unusual combination of caged-structural properties and large diversity of electronic ground states found, e.g., in filled skutterudites [1] and Laves phases [2]. The physical behavior of these systems is mostly dominated by the 4f and 5f electrons and arises from Ruderman-Kittel-Kasuya-Yosida (RKKY) interaction, Kondo effect and crystal-field effects giving rise to many phenomena such as electronic topological (Lifshitz) transitions, heavy-fermion and quantum critical states, superconductivity, magnetic or multi-polar ordering, and many others (for a review see e.g. [3–20]). Wide variety of RT_2M_{20} compounds offers a considerable chemical tunability of their physical properties.

The nonmagnetic subgroup of aluminides RX_2Al_{20} with R = La, Ce, Yb, U, Th, involving the lightest transition metals X = Ti, V, Cr, shows weakly temperature-independent Pauli paramagnetism or diamagnetism. The magnitude of paramagnetic susceptibility depends on the number of the valence electrons [9,17,21–24,26–32]. Electrical resistivity and specific heat measurements showed that all these systems are simple metals with no sign of magnetic order at least down to 0.35 K. This indicates that cerium and ytterbium are in tetravalent and divalent states, respectively, whereas the 5f electrons of uranium are strongly itinerant because of their hybridization with the electronic states of ligands. The behavior of UMn_2Al_{20} distinctly differs from those of all the other RX_2Al_{20} aluminides, namely the compound orders ferromagnetically below 20 K [33]. A dispute about the origin of ferromagnetism in that compound was settled by polarized neutron diffraction study revealing the presence of itinerant magnetic moment only on the manganese sites with no discernible contribution of the uranium atoms [34].

Although many of the non-magnetic RX_2Al_{20} (R = La, Ce, Yb, Th, U; X = Ti, V, Cr) phases have been characterized by means of X-ray diffraction, magnetization, electrical resistivity and heat capacity measurements, to the best of our knowledge only $LaTi_2Al_{20}$, and LaV_2Al_{20} have been studied with a focus on the electronic density of states [17,35]. For the latter compound the Fermi surface has also been calculated using full potential linearized augmented-plane wave (FLAPW) method [22].

* Corresponding author at: Division of Materials Science and Engineering, Ames Laboratory, Ames, Iowa 50011, USA. Department of Physics and Astronomy, Iowa State University, Ames, Iowa 50011, USA.
E-mail address: P.Swatek@int.pan.wroc.pl (P. Swatek).

https://doi.org/10.1016/j.commatsci.2018.06.047
Received 27 February 2018; Received in revised form 29 June 2018; Accepted 30 June 2018

In the present study we calculated the electronic band structures of several RX_2Al_{20} compounds with R = Ce, Yb, Th and U and various X metals. The main aim was at understanding their electronic structure, Fermi surface topology as well as to explore the origin of magnetism in UMn_2Al_{20}, the only ferromagnetic aluminide in the RX_2Al_{20} family.

2. Method of calculations

The electronic structures calculations in the LDA approximation were performed with a FPLO-9.00-34 code [36]. The fully relativistic Dirac equation was solved self-consistently. The Perdew-Wang flavor of the exchange-correlation potential was applied [37] and the energies were converged on a dense k mesh with 12^3 points. For the Fermi surfaces a 64^3 mesh was used to ensure accurate determination of the Fermi level (E_F). The convergence was set to both the density (10^{-6} in code specific units) and the total energy (10^{-8} Hartree). The drawing of the crystal structure was produced with the aid of VESTA [38]. Extremal cross-section areas of the Fermi surfaces were calculated using Mathematica [39].

The structural parameters (unit cell dimensions and atomic coordinates) of (*i*) $LaTi_2Al_{20}$, $CeTi_2Al_{20}$, $YbTi_2Al_{20}$, LaV_2Al_{20}, CeV_2Al_{20}, $LaCr_2Al_{20}$, $CeCr_2Al_{20}$, $YbCr_2Al_{20}$, (*ii*) UTi_2Al_{20}, (*iii*) ThV_2Al_{20}, (*iv*) $ThCr_2Al_{20}$, UCr_2Al_{20} and (*v*) UMn_2Al_{20} were adopted from the reported room-temperature experimental data presented in Refs. (*i*) [24], (*ii*) [40], (*iii*) [41] (*iv*) [30], (*v*) [34], respectively.

Because the atomic positions for (*i*) YbV_2Al_{20} [29], (*ii*) $ThTi_2Al_{20}$ [41] (*iii*) UV_2Al_{20} [33] are unknown, they were assumed to be the same as those derived for (*i*) LaV_2Al_{20} [24], (*ii*) UTi_2Al_{20} [9], (*iii*) ThV_2Al_{20} [41], respectively.

3. Results

3.1. Crystal structure

The crystal structure of RX_2Al_{20}, displayed in Fig. 1a, is a face-centered cubic cell (*f. c. c.*, space group $Fd\bar{3}m$, O_h^7, No. 227), $CeCr_2Al_{20}$-type structure. The unit cell contains 184 atoms located at five different Wyckoff positions [25,42–45]. As apparent from Fig. 2, the unit cell volume decreases significantly when proceeding from X = Ti to Mn, i.e. it follows a decrease in the atomic radius of X-metal.

The cubic unit cell of RX_2Al_{20} can be described as packing of two kinds of Al-based clusters around the R- and X-atoms, namely RAl_{16} and XAl_{12}, shown in Fig. 1a. The R atom is located inside a nearly perfect Frank-Kasper cubic polyhedron made from a truncated tetrahedron by capping the hexagonal faces. It exhibits the point symmetry group $\bar{4}3m$ (T_D). Poor bonding of the R-ion to the neighboring aluminum atoms may give rise to unusually large atomic displacement parameters

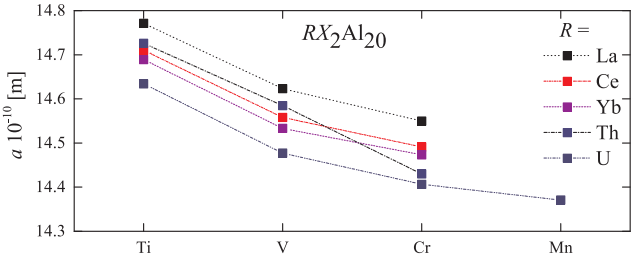

Fig. 2. The experimental lattice parameters of RX_2Al_{20}, where R = La, Ce, Yb, Th and U versus X-3d electron transition metals.

corresponding to anharmonic "rattling" motion about its equilibrium position [17,18].

The transition metal atom, T, has twelve aluminum neighbors occupying vertices of an icosahedron. Since a periodic 3D structure cannot have 5-fold symmetry axes, this icosahedron is slightly (trigonally) distorted and the point symmetry of the T-site is reduced from $m\bar{3}5$ (I_h) to $\bar{3}m$ (D_{3d}) [46,47].

3.2. Electronic structures

The electronic energy band dispersion curves $E(k)$ for RX_2Al_{20} (R = La, Ce, Yb, Th, U) are drawn along the high symmetry lines of k-space in Figs. 3–5. Nearly all bands near the Fermi level demonstrate complex character, including quasi-two-dimensional weakly-dispersive bands, as well as bands with stronger dispersion $dE(k)/dk$ leading to a set of sharp peaks and deep valleys in the density of states (DOS), shown in Figs. 6–8. These bands originate mostly from Al-3p, X-3d and R-f states (Ce-4f, Yb-4f or U-5f).

Total Al-3p contributions shown in Figs. 3–5 create wide and almost featureless bands, mostly at the bottom of the valence band. Many of these bands disperse very weakly along k_x direction and stick together in pairs due to the nonsymmorphic space group.

3.2.1. The d bands

Besides Al-3p and Yb-4f states, the central portion of the valence band is dominated by X-3d states. As shown in Figs. 6 and 9, the Ti-3d-DOS has two distinctive local maxima in the valence band. The lower ones, marked in Fig. 6 by vertical dashed-dotted lines, are centered at about −1.6 eV (R = La, Ce, Yb) and −1.7 eV (R = Th, U) with respect to the Fermi level, E_F. In turn, the upper maxima, marked by dashed lines, are located at about −0.6 eV (R = lanthanide ion) and −0.7 eV (R = actinide ion) below E_F. The empty Ti-3d states in the partial density of states (PDOS) form another structure, somewhat smeared out, with the center of gravity around 2.3 eV above the E_F (note the

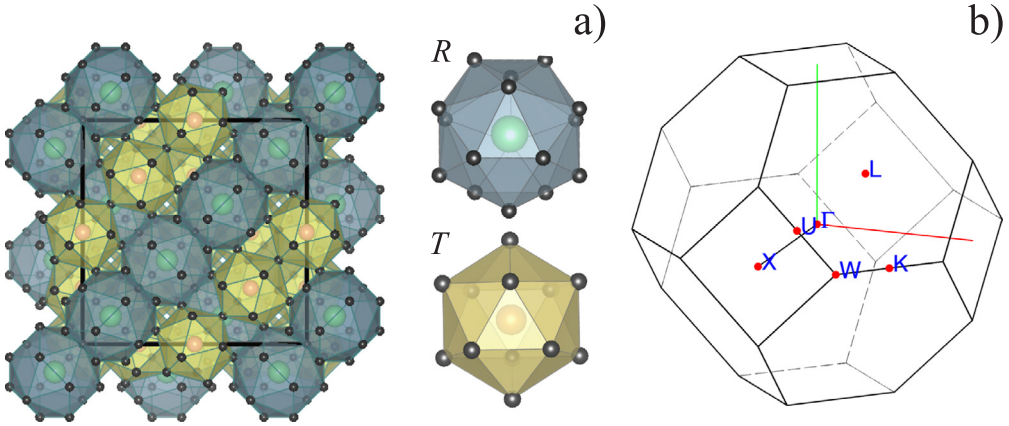

Fig. 1. Left panels: the crystal structure of RX_2Al_{20} shown as a packing of RAl_{16} (shaded in grey) and XAl_{12} (shaded in yellow) clusters. The two polyhedra are presented aside. Right panel: the Brillouin zone for reciprocal-space group $Fd\bar{3}m$.